

In-Situ Copolymerization of Cyclic Poly(butylene terephthalate) Oligomers and ϵ -Caprolactone

Amiya R. Tripathy, William J. MacKnight,* and Stephen N. Kukureka

Polymer Science & Engineering Department, University of Massachusetts, Amherst, Massachusetts 01003

Received March 4, 2004; Revised Manuscript Received June 9, 2004

ABSTRACT: Copolyesters were synthesized by using ring-opening polymerization of cyclic poly(butylene terephthalate) oligomers (c-PBT) and ϵ -caprolactone monomer (CL) in the presence of stannoxane catalyst at an elevated temperature. The in-situ copolymerization was conducted with various c-PBT/CL feed ratios. The copolyesters were characterized by GPC, NMR, and FT-IR techniques. Phase separation and the relaxation behavior of the resultant copolyesters were investigated by DSC, DMTA, and dielectric spectroscopy measurements. Mechanical properties (stress–strain behavior) are also reported and can be adjusted by varying the ϵ -caprolactone content of the copolymer.

Introduction

Conventional semicrystalline engineering thermoplastics, such as poly(butylene terephthalate) (PBT), often have good properties and dimensional stability at elevated temperatures, making them alternatives to thermosetting resins for composites. PBT, however, cannot be processed by traditional means into advanced composites because of its high viscosity. Cyclic oligomers of poly(butylene terephthalate) (c-PBT), on the other hand, have low, water-like viscosity (0.017 Pa s at 190 °C) and are capable of rapid polymerization^{1–6} in the presence of transesterification catalysts (e.g., stannoxane) without the evolution of low-molecular-weight byproducts. This allows for the preparation of highly filled composites having minimal voids and volatile organic compounds. Composites based on in-situ polymerization from low-viscosity c-PBT oligomers could overcome many of the processing problems of the liquid resin molding techniques such as reinforced reaction injection molding (RRIM) and resin transfer molding (RTM).^{7–10}

PBT polymers produced from c-PBT oligomers, using a stannoxane catalyst, undergo crystallization as the polymerization progresses.^{2,3,5,11} The amount of polymer crystallinity can have an effect on the physical properties of the material. This could then affect properties of a reinforced composite system produced from c-PBT. However, it is well-known that copolymerization represents a relatively easy way to modify the characteristics of a polymer in order to fit a specific application by reducing the crystallinity and melting point of the resulting copolymer. To this end, we prepared several polyester copolymers based on ϵ -caprolactone (CL) and c-PBT oligomers via ring-opening copolymerization.⁸

Intensive previous studies have been done on copoly(ether–ester)s based on poly(butylene terephthalate) (PBT) as hard segments and low-molecular-weight polyether soft segments for thermoplastic elastomers. These soft segments include poly(ethylene oxide) (PEO), poly(tetramethylene oxide) (PTMO), poly(ethylene oxide)-*block*-poly(propylene oxide)-*block*-poly(ethylene oxide) (PEO–PPO–PEO), or poly(isobutylene) (PIB)–polyole-

fin copolymers (made using a two-step melt polycondensation between substituted terephthalate, 1,4-butanediol, and the respective soft segments of the copolymer^{12–15}). Du Pont's Hytrel thermoplastic elastomer materials are examples showing the commercial utility of this class of copolymers.

In contrast, c-PBT can be used in thermoset processes to produce thermoplastic elastomers in conjunction with soft segments like ϵ -caprolactone in a single reaction-molding step. Our previous investigation of the in-situ copolymerization of c-PBT and poly(vinyl butyral) (PVB)¹⁶ demonstrates the possibility of producing copolymers with different structures and various physical properties. Interestingly, the above-mentioned PBT thermoplastics, formed by a transesterification reaction, are block copolymers. In the present contribution, we report the production of random copolymers based on c-PBT and CL via in-situ polymerization. The resultant copolymers were characterized by GPC, NMR, FT-IR and WAXD. DSC and DETA studies were performed to provide further understanding of any phase separation between hard and soft segments so that the reasons for the enhanced low-temperature flexibility and good mechanical behavior of the resulting copolymers could be explained.

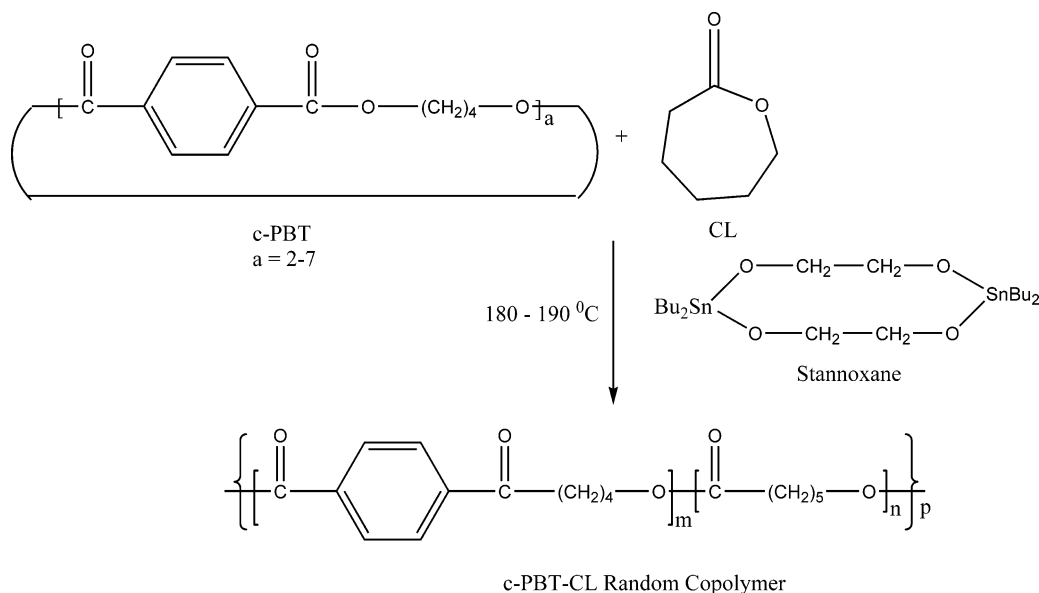
Experimental Section

Materials. ϵ -Caprolactone (CL) was procured from the Aldrich Chemical Co. Cyclic oligomers of poly(butylene terephthalate) (c-PBT) and the stannoxane catalyst were obtained from the Cyclics Corp. CL was dried over calcium hydride (CaH₂), distilled under reduced pressure, and stored over activated 4 Å molecular sieves. c-PBT copolymer was dried in a vacuum oven for about 20 h at 80 °C.

Synthesis of in-Situ c-PBT/CL Copolymers. The required amounts (2 g of c-PBT/CL, w/w) of previously dried c-PBT copolymers and CL were placed in a vial equipped with a magnetic bar and sealed with a Teflon septum. The vial was flushed with dry nitrogen gas for about half an hour; then it was placed in a silicone oil bath, and the temperature was increased to 160 °C over 8–10 min under constant stirring. On reaching this temperature and after a further 2–3 min of stirring, some previously dissolved stannoxane catalyst (0.05 g or 0.025 wt % of the reactants) in a small amount of anhydrous toluene was injected rapidly into the reactant mixture in the vial. The stirring was then continued for

* Corresponding author: e-mail wmacKnight@polysci.umass.edu.

Scheme 1



another 3 min at 160 °C so that the catalyst was mixed properly into the mixture. Subsequently, the temperature was allowed to rise to 185–190 °C by increasing the oil bath temperature within 2–3 min along with a gentle dry N₂ purge under constant stirring so that toluene would be removed, and the polymerization reaction resumed. Stirring was stopped automatically because of the polymerization and subsequent crystallization of the polymer in the vial. After 3 min of the reaction the vial along with the contents was placed in an ice bath for about 2–3 min. The N₂ purge was stopped, and finally the polymer (Scheme 1: due to the ring-opening nature of the ϵ -caprolactone polymerization, we assume that the random copolymer depicted in Scheme 1 is linear) was vacuum-dried at 80 °C for 12 h. It was characterized without any further purification.

Characterization. a. Gel Permeation Chromatography. The number-average molecular weight (M_n), weight-average molecular weight (M_w), and polydispersity index (M_w/M_n) were obtained using gel permeation chromatography (GPC). The GPC was performed on a modular system comprising a Waters 590 HPLC pump, a Waters 717 autosampler, and an ERMA ERC-7515A refractive index detector (ERMA CR, Inc., Tokyo). The mobile phase was unstabilized CHCl₃ at a flow rate of 0.95 mL/min at 30 °C. The molecular weights were calculated using 13 narrow polystyrene standards from 6 300 000 to 580 g/mol (Pressure Chemical Co., Pittsburgh, PA). The copolymers were dissolved in CHCl₃; c-PBT homopolymer and c-PBT/CL (90/10) copolymers were dissolved in a mixture of chloroform/dichloromethane/1,1,1,3,3,3-hexafluoro-2-propanol (HFIP) [60/30/10 v/v/v] (details are in the Results and Discussion section).

b. NMR Spectra. Structural characterization of the copolymers was performed using ¹³C and ¹H NMR spectroscopies. Spectra were collected on a Bruker DPX 300 spectrometer using 5 mm o.d. tubes and deuterated chloroform as a solvent for the copolymers. A solvent mixture of chloroform-*d*/dichloromethane-*d*₂/1,1,1,3,3,3-hexafluoro-2-propanol-*d*₂ (HFIP-*d*₂) [60/30/10, v/v/v] was used for the c-PBT homopolymer and c-PBT/CL (90/10) copolymers only. Sample concentrations were 30–35% (w/v) for ¹³C and 6–8% (w/v) for ¹H NMR spectra.

c. Fourier Transform Infrared Spectra (FT-IR). Fourier transform infrared spectra were obtained on an IBM IR44 FTIR spectrometer. A total of 128 scans at a resolution of 1 cm^{−1} were signal-averaged. Except for the c-PBT homopolymer and c-PBT/CL (90/10) copolymer [dissolved in a mixture of HFIP, CH₂Cl₂, and CHCl₃ (10/30/60, v/v/v) as above], all copolymer samples were dissolved in CHCl₃. The solutions were directly cast on a KBR window under a slow stream of nitrogen. The concentrations of the solutions ranged from 4

to 6% (w/v). Spectra were taken from 5000 to 400 cm^{−1} in the transmission mode using a NB-MCT detector.

d. DSC Study. Differential scanning calorimetry (DSC) was performed on a TA Instruments machine calibrated with indium. Experiments were run with samples ranging from 10 to 15 mg under dry nitrogen to prevent moisture and oxidative degradation. Samples were subjected to the following heating and cooling steps: (a) first heated to 250 °C, equilibrated at 250 °C, and kept for 5 min at 250 °C; (b) rapidly cooled to −80 °C, equilibrated at −80 °C, and kept for 5 min at −80 °C; and (c) heated to 250 °C at a 10 °C/min heating rate. The results of the last step are presented in Figure 4. Crystallinity of the homopolymers has been calculated according to the following relation and tabulated in Table 4:

$$X_c (\%) = (\Delta H_f / \Delta H_f^0) \times 100$$

where ΔH_f is the measured heat of fusion for the sample and ΔH_f^0 is the heat of fusion for 100% crystalline polymer. According to the work published earlier, the heat of fusion of 100% crystalline PCL is 135 J/g¹⁷ and that of PBT is 85.75 J/g.¹⁸ The relative contributions to the heat of fusion for the respective copolymers have been calculated as per weight ratios of PCL and c-PBT, respectively, depending on the crystal structure in the resultant copolymer (as obtained from the WAXD, Figure 6).

e. Dynamic Mechanical Thermal Analysis (DMTA). Dynamic mechanical thermal analysis was performed by using TA Instruments DMA 2980 dynamic mechanical analyzer in a tension mode with solution-cast film samples of dimensions 12 mm × 6 mm × 1 mm. The lower limit of the dynamic temperature scan was fixed at −90 °C, and the upper limit was selected 30 °C below the melting temperature (obtained from the DSC curves, Figure 4) of each polymer so that relaxation due to melting of the polymer can be avoided. The heating rate was 5 °C/min, and the frequency was fixed at 1 Hz.

f. Wide-Angle X-ray Diffraction (WAXD). Wide-angle X-ray diffraction data were collected on a D500 Siemens diffractometer using Cu K α (40 kV, 35 mA) radiation and a secondary beam graphite monochromator. The spectra were recorded in the 2 θ range from 2° to 40° in steps of 0.08° and a counting time per step of 1 s. Data are presented in normalized intensity (to remove any thickness problem of the copolymers) vs “ $q = (4\pi) \sin \theta / \lambda$ ” at room temperature in Figure 6. Crystallinity and the d spacing of the polymers have been reported in Table 5, considering the PBT¹⁹ as triclinic and polycaprolactone²⁰ as orthorhombic crystal structures.

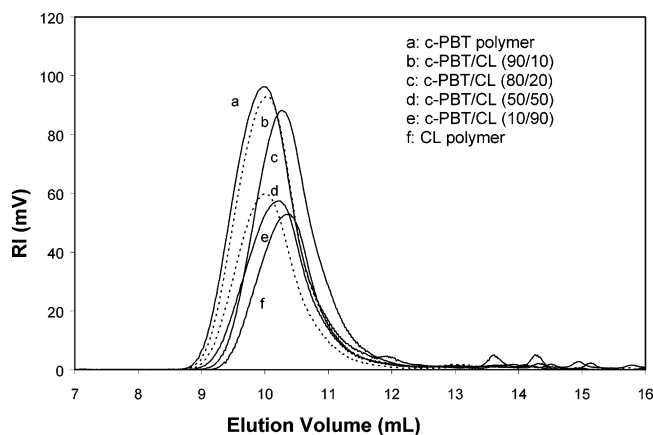


Figure 1. GPC chromatograms of in-situ polymerized c-PBT/CL polyesters.

g. Dielectric Measurements. Measurements of the complex dielectric function were made with a Novocontrol BDC-S system composed of a frequency response analyzer (Solartron Schlumberger FRA 1260), a broadband dielectric converter, and an active sample cell containing six reference capacitors from 25 to 1000 pF. Measurements were made over a frequency range from 0.1 to 10^6 Hz. The samples were kept between two gold-plated stainless steel plates of 20 mm diameter with a separation of 100 mm, resulting in a sample capacitance of about 100 pF. Samples (about 26 mm diameter) were gold-plated to about 300 nm thickness on both sides prior to measurements. Care was taken so that the samples completely filled the capacitor cell. The lower temperature of the samples was fixed at -100 °C, and the upper one was varied depending on the melting peak obtained from the DSC (20 °C less than the respective melting temperature).

h. Mechanical Properties. The mechanical behavior of the copolyester samples was analyzed using an Instron model 5568. Test specimens were made from solution-cast films (~30 mm length, 6 mm width, and 0.5 mm thickness). The stress-strain curves were obtained at room temperature at a cross-head speed of 18 mm/min. Young's modulus was calculated from the initial slope at 3–4% strain. Mechanical tensile data were averaged over at least four specimens.

Results and Discussion

At room temperature c-PBT/CL copolymers are semicrystalline solids. c-PBT homopolymer and copolymers with compositions greater than 80 wt % of butylene terephthalate units are soluble at room temperature in HFIP and in a mixture of chloroform/dichloromethane/HFIP (60/30/10 v/v/v). Copolymers of CL-rich material and c-PBT/CL below 80/20 (w/w) copolymer are completely soluble in chloroform at room temperature.

The GPC traces for homopolymers of c-PBT, CL, and c-PBT/CL copolymers, shown in Figure 1, exhibit a single peak, which differs in magnitude and elution volume between samples. Pure c-PBT homopolymer has a maximum at 9.8 mL of eluted volume, whereas PCL homopolymer reaches a maximum at 10.7 mL and copolymers of c-PBT and CL attain a maximum between 9.8 and 10.7 mL depending on the amount of c-PBT and CL in the copolymers. It is also observed that the maximum shifts to lower values with increasing quantities of CL units in the copolymer. The low-molecular-weight tail (between 13.5 and 16 mL of eluted volume) is quite small, thus suggesting that the low-molecular-weight oligomers are not very abundant and that the yields of polymer are more than 95%. The weight-average molecular weights roughly estimated through a polystyrene calibration curves are shown in

Table 1. Molecular Weights and Polydispersity Index of c-PBT/CL Copolyesters

sample	M_n [g/mol] $\times 10^4$	M_w [g/mol] $\times 10^4$	M_w/M_n
c-PBT polymer	3.97	11.8	2.9
c-PBT/CL (90/10)	4.92	11.5	2.3
c-PBT/CL (80/20)	2.90	7.22	2.4
c-PBT/CL (60/40)	3.12	6.84	2.2
c-PBT/CL (50/50)	4.77	11.0	2.3
c-PBT/CL (10/90)	3.08	8.65	2.8
PCL	2.94	6.11	2.0

Table 1. The number-average molecular weight varies between 30 000 and 40 000, and the polydispersity index remains approximately "2"²¹ in all cases. In addition, by increasing the amount of c-PBT, the molecular weight distribution narrows, which is characteristic of a ring-opening polymerization process in the presence of stannoxane catalyst.²²

The chemical structure of all the polyesters was determined by FTIR and the NMR spectral analysis. The characteristic stretching frequencies of the ester groups appear at 1724 cm^{-1} ($\nu_{\text{C=O}}$) and 1191 cm^{-1} ($\nu_{\text{C-O}}$) for polycaprolactone. For c-PBT polymer they occur at 1714 cm^{-1} ($\nu_{\text{C=O}}$), 1118 cm^{-1} ($\nu_{\text{C-O}}$ aliphatic end), and 1103 cm^{-1} ($\nu_{\text{C-O}}$ aromatic end), as shown in Table 2. Upon copolymerization, due to the transesterification reaction the stretching frequencies in 50/50, 60/40, and 70/30 (w/w) c-PBT/CL copolymers are shifted: for carbonyl ($\nu_{\text{C=O}}$) to 1717, 1716, and 1715 cm^{-1} ; for the $\nu_{\text{C-O}}$ frequency of PCL units to 1165, 1166, and 1169 cm^{-1} ; and for $\nu_{\text{C-O}}$ frequency of c-PBT units to 1119 and 1104 cm^{-1} , respectively.

The ^1H NMR spectra of all copolyesters are shown in Figure 2, and the chemical shifts are tabulated in Table 3. The ^1H NMR spectra were obtained from solution using deuterated chloroform as a solvent. Pure c-PBT homopolymer does not dissolve in CHCl_3 . Therefore, it is expected that the behavior of PCL alone is reflected in the spectra as PCL is fully soluble in CHCl_3 . Numbers 1–5 denote carbons in the PBT units, and Greek symbols α – ϕ indicate the carbons in the CL units (Chart 1). A triplet at 4.05 ppm is assigned to the ϵ -methylene proton attached to $-\text{O}-$, a triplet at 2.3 ppm for the α -methylene proton attached to $-\text{C=O}$, and multiplets at 1.6 and 1.4 ppm are assigned to β , δ , and γ methylene protons, respectively, in CL units.²³ Peaks at 8.09 ppm are due to aromatic protons (C_2 – C_3); those at 4.41 ppm are assigned to the methylene proton (C_4) attached to the $-\text{O}-$ in the ester groups and at 1.19 ppm for the methylene unshielded proton (C_5) of the PBT unit. This indicates that the PBT unit is present in the copolyesters. Further, the presence of several peaks corresponding to the chemical shifts at 4.05 ppm (H_ϵ protons) and 4.41 ppm (H_4 protons) for 70/30 and 40/60 c-PBT/CL copolymers suggests a mixture of various protons of the c-PBT/CL random copolymer.

It is to be noted at this stage that the reaction between c-PBT oligomers and the ϵ -caprolactone in the presence of stannoxane catalyst is a transesterification reaction, and ^{13}C NMR is more suitable for detecting C–H connectivity directly with a wide chemical shift range to resolve each peak easily. Details of the peak assignment of ^{13}C NMR (Figure 3) are given in Table 3. Samples were dissolved in CDCl_3 unless otherwise noted. Chemical shifts: 173 ppm for $-\text{C=O}$ carbon (C_ϕ), 63 ppm for $\text{CH}_2-\text{O}-$ (C_ϵ), downfield shifts at 33 for C_α , 27 for C_β , 25 for C_δ , and 24 ppm for C_γ carbons in CL units are observed in polyesters. Chemical shifts at 168

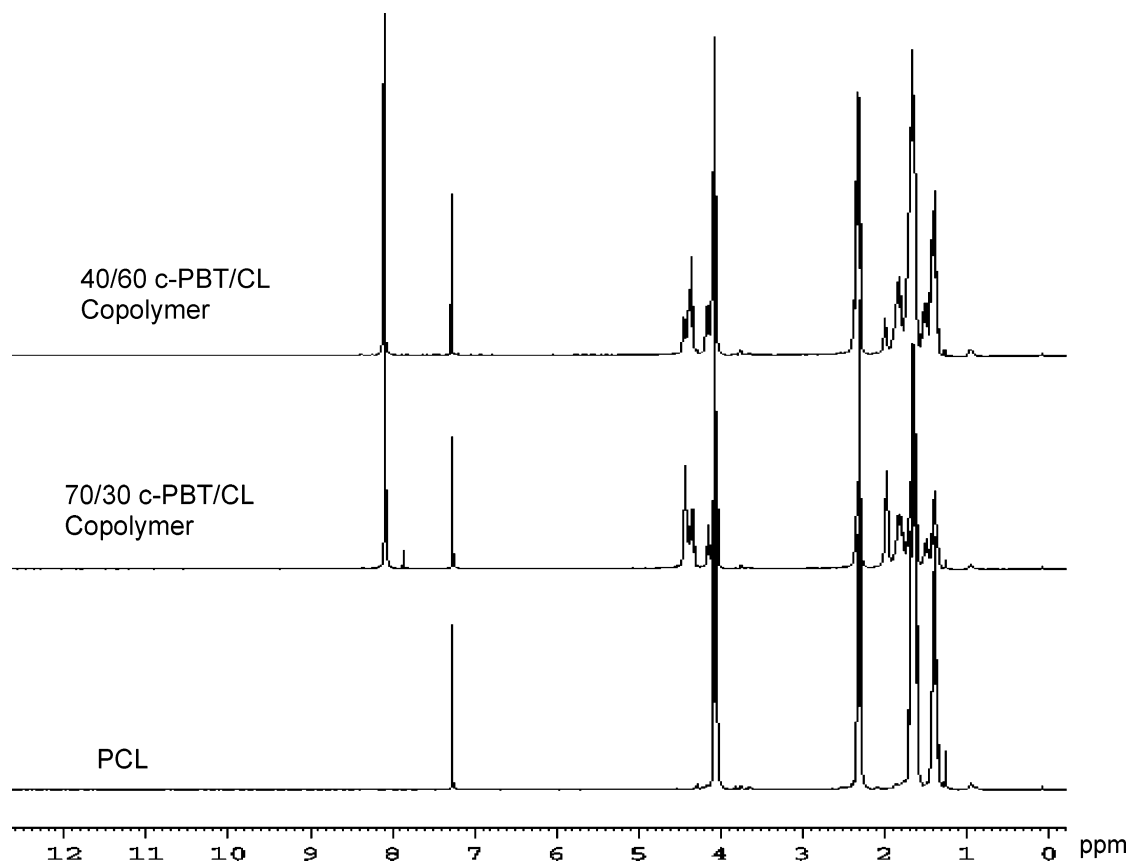


Figure 2. ^1H NMR spectra of in-situ polymerized polyesters.

Table 2. Shifting in FT-IR Stretching Frequencies in the in-Situ Copolyesters

sample	$\nu_{\text{C=O(PCL)}} (\text{cm}^{-1})$	$\nu_{\text{C=O(PBT)}} (\text{cm}^{-1})$	$\nu_{\text{CH}_2(\text{PCL})} (\text{cm}^{-1})$	$\nu_{\text{CH}_2(\text{PBT})} (\text{cm}^{-1})$	$\nu_{\text{C-O(PCL)}} (\text{cm}^{-1})$	$\nu_{\text{C-O(PBT)}} (\text{cm}^{-1})$
PCL	1724		2944		1191	
c-PBT polymer		1714		2962		1118, 1103
c-PBT/CL (50/50)	1717	1717	2951	2951	1165	1119, 1104
c-PBT/CL (60/40)	1716	1716	2954	2954	1166	1119, 1104
c-PBT/CL (70/30)	1715	1715	2960	2960	1169	1119, 1104

Table 3. Chemical Shifts for ^{13}C and ^1H Species in c-PBT/CL in-Situ Copolyesters by NMR

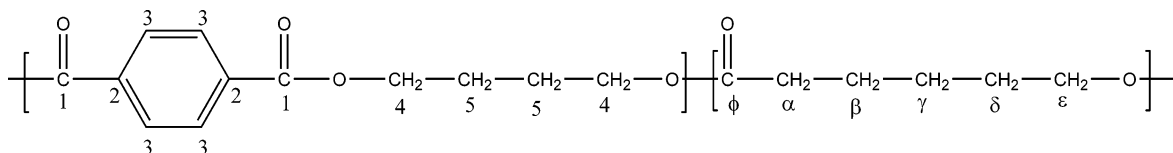
^{13}C	chemical shift (ppm)	^1H	chemical shift (ppm)
C_ϕ	173	H_3	8.09
C_ϵ	63	H_4	4.41
C_α	33	H_5	1.95
C_β	25	H_ϵ	4.05
C_γ	24	H_α	2.3
C_δ	28	$\text{H}_\beta, \text{H}_\delta$	1.6
C_1	168	H_γ	1.4
$\text{C}_2\text{--C}_3$	133–128		
C_4	65		
C_5	24		

ppm are due to C=O (C_1), downfield shifts at 133 and 128 ppm are assigned to aromatic C_2 and C_3 carbon atoms, and chemical shifts at 65 and 24 ppm are for C_4 and C_5 carbon atoms in the PBT units. Therefore, copolyesters soluble only in CDCl_3 confirm that the copolymers consist of PBT and CL units. Also, ^{13}C NMR (Figure 3) of pure PCL homopolymer in CDCl_3 and pure

c-PBT homopolymer in a mixture of chloroform- d_2 /dichloromethane- d_2 /HFIP- d_2 (60/30/10, v/v/v) shows similar peaks of $\text{C}_\alpha\text{--C}_\phi$ in the CL unit and $\text{C}_1\text{--C}_5$ in the PBT unit, respectively. The presence of few peaks corresponding to the chemical shifts at 33 ppm for C_ϵ carbons and 63 ppm for C_α carbons in 70/30 and 40/60 c-PBT/CL copolymers indicates the mixture of various aliphatic carbons because of the formation of the random copolymer. Evidence of formation of the c-PBT/CL random copolymer in our present experimental condition out of c-PBT oligomers, and CL is discussed further in the following sections.

The copolyesters were also examined by differential scanning calorimetry (DSC) (Figure 4). The onset of the PBT melting point decreases (Table 4) along with a broadening of the peak with increasing CL content in the copolyesters, indicating a broadening of the crystallite size distribution. These observations are typical for random copolymers in which only one of the constituents has sequence lengths long enough to allow

Chart 1



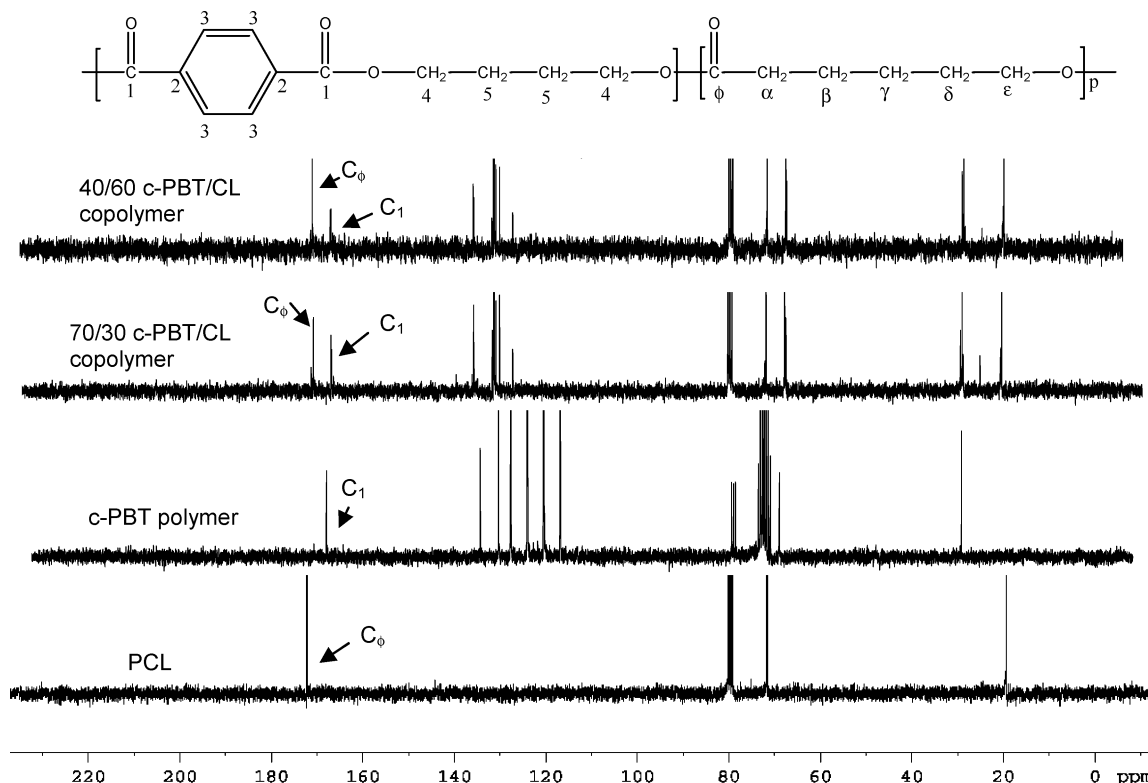


Figure 3. ^{13}C NMR spectra of in-situ polymerized polyesters.

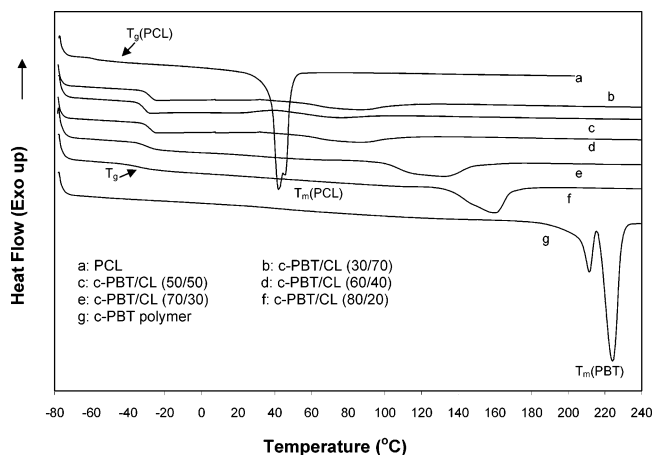


Figure 4. DSC thermogram of in-situ polymerized polyesters.

crystallization to take place. In the present case, an examination of Figure 6 (WAXD) shows that all the c-PBT-rich copolymers and the compositions containing 50 wt % of each constituent exhibit the PBT crystal structure. The copolymer containing 30 wt % of c-PBT exhibits the PCL crystal structure. Thus, it appears that PCL sequences are not long enough to form crystalline domains in the copolymers with 50% or greater PBT content. A T_g for the c-PBT homopolymer cannot be seen because of its highly crystalline nature, but copolymers clearly show a T_g at around $-30\text{ }^\circ\text{C}$, which varies with CL content (see Table 4). It is very interesting that, at elevated temperature in the presence of stannoxane catalyst, CL monomer reacts faster than the c-PBT oligomer. (This observation was noted in separate polymerizations of pure CL.) Therefore, the existence of long PCL sequences in above copolymers is favored over the presence of long PBT sequences. However, the broad melting peaks and distinct glass transition tem-

peratures in the copolymers suggest that the copolymers do not contain long sequences of either CL or PBT, probably due to the transesterification noted above. The crystallinity of the homopolymers of c-PBT and CL polymers have been calculated (shown in Table 4) from their respective heats of fusion. However, the crystallinities of the copolymers have been calculated (Table 4) from the WAXD (Figure 6, discussed in the following section).

Further evidence for the absence of long sequences of either CL or c-PBT in the c-PBT/CL copolymers comes from the DMTA study (Figure 5). Shown is the loss modulus E'' for the copolymers as a function of temperature for the series of different compositions of c-PBT and CL. The copolymers of c-PBT/CL show a single relaxation peak associated with the T_g irrespective of the copolymer compositions. The relaxation peaks corresponding to either c-PBT polymer or CL polymer in the in-situ copolymerized copolymers are absent. It means that none of the copolymers are phase-separated under our polymerization conditions. This confirms that neither the c-PBT nor the CL is present as long sequences in the resultant copolymers. It is also noted that the loss modulus peak position ($-46\text{ }^\circ\text{C}$ for CL polymer, $-39\text{ }^\circ\text{C}$ for 30/70 c-PBT/CL, $-29\text{ }^\circ\text{C}$ for 50/50 c-PBT/CL, $-25\text{ }^\circ\text{C}$ for 60/40 c-PBT/CL, $-7\text{ }^\circ\text{C}$ for 70/30 c-PBT/CL, $-1\text{ }^\circ\text{C}$ for 80/20 c-PBT/CL copolymers, and $78\text{ }^\circ\text{C}$ for c-PBT polymer) corresponding to the T_g of the copolymers gradually shifts toward higher temperatures and finally broadens as the c-PBT content increases (Figure 5). As discussed in the literature,²⁴ the relaxation corresponding to the T_g usually broadens and moves to higher temperature with increasing crystallinity in polyesters. This behavior is particularly notable in the samples with high PBT content, which correspond to the most crystalline materials.

Table 4. DSC Data of c-PBT/CL Copolyesters

sample	T_g (°C)	$T_{s,onset}$ (°C)	$T_{s,max}$ (°C)	ΔH_{fusion} (J/g)	% crystallinity
c-PBT polymer	40	216	224	57.36	67
c-PBT/CL (80/20)	-33	131	178.5	51.33	59
c-PBT/CL (70/30)	-30	95	131	45	52
c-PBT/CL (60/40)	-28	89	114	26.8	31
c-PBT/CL (50/50)	-31	74	119	22.6	26
c-PBT/CL (10/90)	-58	38	42	58.6	43
PCL	-62	49	53	73.6	54

Table 5. Crystallinity and d Spacing of c-PBT/CL Copolymers from WAXD

polymers	crystallinity (%)	d spacing (Å)							
c-PBT polymer	68	$d_{001} = 9.9882$	$d_{010} = 5.4735$	$d_{002} = 5.1418$	$d_{200} = 4.2636$	$d_{011} = 3.7836$	$d_{100} = 3.5403$	$d_{101} = 3.059$	
(70/30) cPBT/CL copolymer	49		$d_{010} = 5.3767$	$d_{002} = 5.0080$	$d_{200} = 4.2082$	$d_{011} = 3.7499$	$d_{100} = 3.4628$	$d_{101} = 2.843$	
(60/40) cPBT/CL copolymer	35		$d_{010} = 5.3758$	$d_{002} = 4.9919$	$d_{200} = 4.1972$	$d_{011} = 3.7516$	$d_{100} = 3.4697$	$d_{101} = 3.0445$	
(50/50) cPBT/CL copolymer	28		$d_{010} = 5.5743$	$d_{002} = 5.1590$	$d_{200} = 4.368$	$d_{011} = 3.88$	$d_{100} = 3.5844$		
(30/70) cPBT/CL copolymer	44			$d_{102} = 5.879$	$d_{110} = 4.4658$	$d_{111} = 3.954$	$d_{201} = 3.1052$		
PCL	56		$d_{101} = 6.6112$	$d_{102} = 5.4933$	$d_{110} = 4.0917$	$d_{111} = 3.953$	$d_{201} = 3.6767$	$d_{211} = 2.9501$	

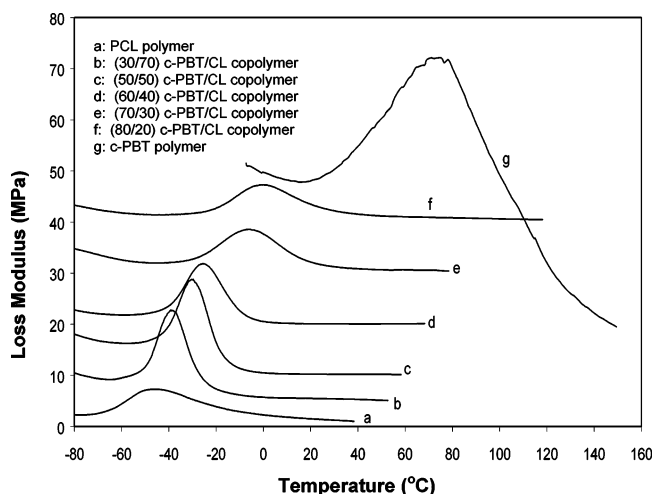


Figure 5. Dynamic loss modulus vs temperature of in-situ polymerized polyesters.

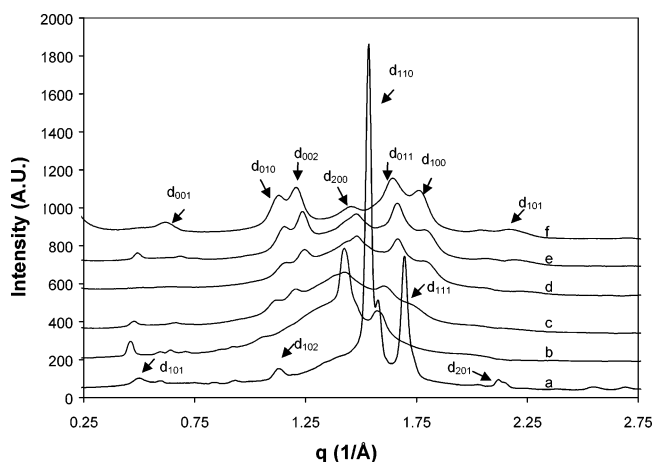


Figure 6. Wide-angle X-ray diffraction of in-situ polymerized polyesters.

A normalized wide-angle X-ray scattering intensity WAXS plot for the copolymers is plotted against " q " [$(4\pi/\lambda) \sin \theta$] in Figure 6. The poly(caprolactone) homopolymer has a pronounced maximum at $q = 1.52$ ($1/\text{\AA}$), corresponding to a d spacing (d_{110}) of 4.09 Å.²⁵ The c-PBT scattering profile shape is similar to the linear PBT pattern^{26,27} typical of a semicrystalline polymer. The diffraction patterns of the c-PBT-rich copolymers are very similar to those of c-PBT homopolymer. These results show that the crystal structure develops in the

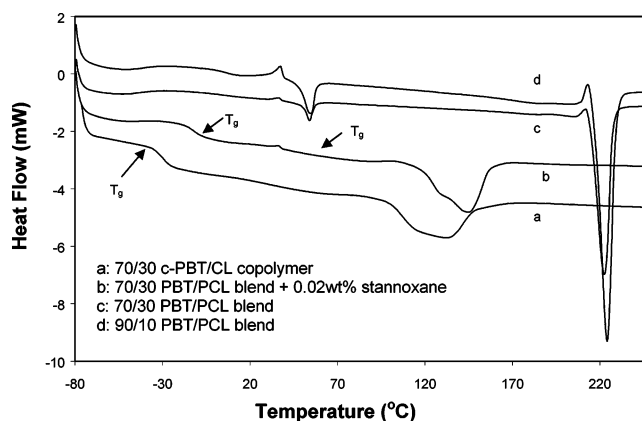


Figure 7. DSC thermogram of PBT/PCL blend.

above copolymers corresponds to the characteristic lattice of a c-PBT polymer. The only difference is an increasing amount of amorphous material and reduced crystal size with increasing amount of CL in the copolymers. Table 5 reveals that the d spacing of the most prominent peaks in the c-PBT copolymers have been reduced gradually up to (50/50) c-PBT/CL ratio. In the WAXS of the CL-rich copolymer, the profile is similar to that of PCL with an increased d spacing value in comparison with d spacing in PCL. This suggests that all CL-rich copolymers crystallize in a similar way to PCL homopolymer.

Figure 6 indicates that all the copolymers from pure c-PBT polymer to the 50/50 compositions appear to possess the PBT crystal structure. The 30/70 c-PBT/CL polymer has the PCL crystal structure with the main peaks reduced in intensity and moved to smaller q (increased d spacing) compared to pure PCL. This shows that only one copolymer component crystallizes, indicating that the sequence lengths of the other component are of insufficient length to crystallize.

To distinguish between the blends and copolymers of PBT and PCL, we blended PBT and PCL ($M_w = 16$ 000) in a twin-screw extruder at 235 °C for 5 min with and without a transesterification catalyst (here stannoxane). The DSC curves (Figure 7) of PBT/PCL blends of 70/30 and 90/10 (w/w) show two distinct melting peaks corresponding to PCL (54 °C) and PBT (225 °C) polymers. The blend of 70/30 PBT/PCL in the presence of 0.02 wt % stannoxane shows two T_g s at -10 and 37 °C (amorphous PBT) and a broad melting peak instead of two distinct melting peaks corresponding to PBT and PCL

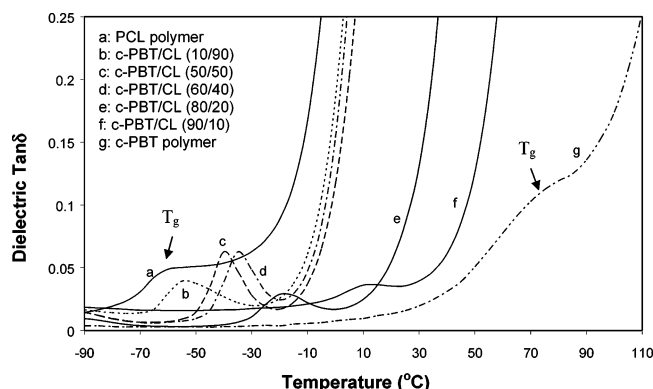


Figure 8. Dielectric $\tan \delta$ vs temperature of in-situ polymerized polyesters at 50 Hz.

polymers (Figure 7), suggesting compatibility as reported by many authors.^{28–32} On the other hand, we see a single T_g (-29°C) along with a broad melting peak in the 70/30 c-PBT/CL copolymer (Figures 4 and 7).

The WAXS profile of the copolymers (Figure 6) may also be used to estimate the degree of crystallinity from the relative areas under the crystalline peaks and the amorphous halo. Using peak separation software, the respective crystalline and amorphous areas have been calculated, and the crystallinity has been determined from their ratio and tabulated in Table 5. The values thus obtained from the WAXD profiles (Figure 6) compare reasonably well with those obtained from the DSC (Table 4). The crystallinity of PCL is about 56%, which is comparable to the literature values³³ (Tables 4 and 5). The crystallinity of c-PBT homopolymer is about 68% (Tables 4 and 5), which is slightly higher than reported for conventional PBT.^{3,26,27}

As both c-PBT and CL are polar species, the resultant copolymers are expected to be dielectrically active. Therefore, the response in an applied electric field due to permanent dipoles present in the copolymers with variation of temperature and frequency can be monitored as a probe for the structural heterogeneity of the copolymer. Figure 8, for measurements at a constant frequency of 50 Hz, shows a single dielectric $\tan \delta$ peak over the temperature range investigated in each copolymer corresponding to a relaxation process associated with the presence of a single glass transition. The peak temperature corresponding to the T_g for c-PBT homopolymer is 78°C , and that for PCL is -62°C (Figure 8). As the temperature rises, the loss curve becomes broader on the high-temperature side (Figure 8). This behavior is also consistent with the dynamic mechanical relaxation results. Both homopolymers show broad loss peaks, somewhat obscured by the onset of dc conductivity in the dielectric results. The copolymers of intermediate composition are lower in crystallinity and exhibit narrower, better defined dielectric and mechanical loss peaks than the homopolymers.

Mechanical testing was performed on solution-cast test samples with an average thickness of 0.5 mm and width 6.5 mm (Table 6). The stress-strain behavior (Figure 9) is typical of ductile materials—a yield point, necking, and strain hardening until fracture. All of the copolymers failed in a ductile manner with yielding and a high elongation at break. Pure PCL polymer fractures in a brittle fashion with a very low elongation at break. c-PBT-rich copolymers show yield and a maximum stress at break along with a high elongation. Cold drawing with limited strain hardening was observed in

Table 6. Mechanical Properties of c-PBT/CL Copolyesters

sample	Y (GPa)	σ_Y (MPa)	σ_B (MPa)	ϵ_B (%)
PCL	28.6×10^{-2}	14.85	12.6	25
c-PBT/CL (30/70)	0.04×10^{-2}	0.79	3.6	820
c-PBT/CL (50/50)	1.8×10^{-2}	2.4	5.3	690
c-PBT/CL (60/40)	4.9×10^{-2}	5.05	8.2	397
c-PBT/CL (70/30)	16.6×10^{-2}	13.2	18.9	704
c-PBT/CL (80/20)	5.7×10^{-2}	9.3	13.9	368

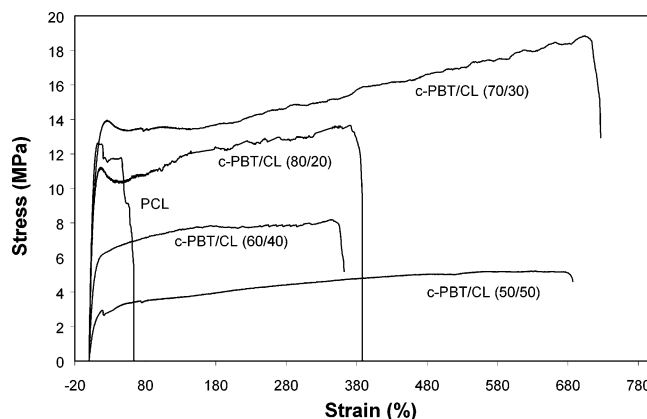


Figure 9. Stress-strain curve of in-situ polymerized polyesters.

the CL-rich copolymers. By contrast, c-PBT-rich copolymers show strain hardening prior to failure. The Young's modulus (E), yield stress (σ_Y), and the stress at break (σ_B) exhibit an increase with c-PBT concentration in the copolymers, but (80/20) c-PBT/CL copolyester shows a decrease (Table 6). As above, elongation at break increases without any increase in tensile stress with an increase in CL content in the polyesters. In the case of c-PBT-rich copolymers a prominent yield point with a very high yield stress occurs (Figure 9, Table 6).

Conclusions

Cyclic oligomers of PBT have successfully been copolymerized in situ with ϵ -caprolactone in the presence of a stannoxane catalyst. The synthesized copolymers exhibit a range of thermal properties from very low glass transition temperature (-30°C) to high melting temperature dependent on c-PBT content, which makes them candidates for applications over broad temperature ranges. Copolymers of c-PBT/CL are dielectrically active over a wide range of frequency, as observed by DETA. The mechanical properties, such as Young's modulus, yield stress, and stress at break, can be adjusted by varying the ϵ -caprolactone amount in the copolymers. Most importantly, the typical brittle nature of solvent-cast c-PBT polymers can be eliminated by the incorporation of a small amount of CL.

Acknowledgment. Support from Cyclics Corp., Schenectady, NY, and the National Environmental Technology Institute (NETI) is gratefully acknowledged. We thank Cyclics Corp. for providing samples.

References and Notes

- (1) Brunelle, D. J. U.S. Patent 5,498,651, 1996.
- (2) Brunelle, D. J.; Bradt, E. J.; Guzzo, J. S.; Takekoshi, T.; Evans, T. L.; Pearce, E. J.; Wilson, P. R. *Macromolecules* **1998**, *31*, 4782.
- (3) Miller, S. *Macrocyclic Polymers from Cyclic Oligomers of Poly-(butylene terephthalate)*. Ph.D. Dissertation, University of Massachusetts, 1998.

- (4) Youk, J. H.; Kambour, R. P.; MacKnight, W. J. *Macromolecules* **2000**, *33*, 3594.
- (5) Youk, J. H.; Kambour, R. P.; MacKnight, W. J. *Macromolecules* **2000**, *33*, 3600.
- (6) Youk, J. H.; Kambour, R. P.; MacKnight, W. J. *Macromolecules* **2000**, *33*, 3606.
- (7) Brunelle, D. J. U.S. Patent 5,648,454, 1997.
- (8) Wang, Y. F. U.S. Patent 6,420,048, 2002.
- (9) Winckler, S. J.; Takekoshi, T. U.S. Patent 6,369,157, 2002.
- (10) Astrom, B. *Polymer Composites Manufacturing*; 1996.
- (11) Bahr, S. R. Personal communication.
- (12) Adams, R. K.; Hoeschele, G. K.; Witseipe, W. K. In *Thermoplastic Elastomers*; Holden, G., Legge, N. R., Quirk, R., Schroeder, H. E., Eds.; Hanser: Munich, 1996.
- (13) Hoeschele, G. K.; Witsiepe, W. K. *Angew. Makromol. Chem.* **1973**, *29/30*, 267.
- (14) Schmalz, H.; Abetz, V.; Lange, R.; Soliman, M. *Macromolecules* **2001**, *34*, 795.
- (15) Cella, R. J. *J. Polym. Sci., Polym. Symp.* **1973**, *42*, 727.
- (16) Tripathy, A. R.; Chen, W.; Kukureka, S. N.; MacKnight, W. J. *Polymer* **2003**, *44*, 1835.
- (17) Crescenzi, V.; Manzini, G.; Calzolari, G.; Borri, C. *Eur. Polym. J.* **1972**, *8*, 449.
- (18) Boutevin, B.; Khamlichi, M.; Pietrasanta, R. J. *J. Appl. Polym. Sci.* **1995**, *55*, 191.
- (19) Yokouchi, M.; Sakakibara, Y.; Chatani, Y.; Tadokoro, H.; Tanaka, T.; Yoda, K. *Macromolecules* **1976**, *9*, 266.
- (20) Chatani, Y.; Okita, Y.; Tadokoro, H.; Yamashita, Y. *Polym. J.* **1970**, *1*, 555.
- (21) Lotti, N.; Finelli, L.; Siracusa, V.; Munari, A.; Gazzano, M. *Polymer* **2002**, *43*, 4355.
- (22) Montaudo, G.; Montaudo, M. S.; Puglisi, C.; Samperi, F.; Spassky, N.; LeBorgne, A.; Wisniewski, M. *Macromolecules* **1996**, *29*, 6461.
- (23) Storey, R. F.; Taylo, A. E. *J. Macromol. Sci., Pure Appl. Chem.* **1996**, *A33*, 77.
- (24) Rabek, J. F. *Experimental Methods in Polymer Chemistry*; John Wiley & Sons: New York, 1980.
- (25) Bgitter, H.; Marchessault, R. H.; Niegisch, W. D. *Acta Crystallogr.* **1970**, *B26*, 1923.
- (26) Mencik, Z. *J. Polym. Sci., Polym. Phys.* **1975**, *13*, 2173.
- (27) Lotti, N.; Finelli, L.; Siracusa, V.; Munari, A.; Gazzano, M. *Polymer* **2002**, *43*, 4355.
- (28) Porter, R. S.; Wang, L. *Polymer* **1992**, *33*, 2019.
- (29) Suzuki, T.; Tamaka, T.; Nishi, T. *Polymer* **1989**, *30*, 1287.
- (30) Nishi, T.; Suzuki, T.; Tamaka, H.; Hayashi, T. *Makromol. Chem., Macromol. Symp.* **1991**, *51*, 29.
- (31) Devaux, J.; Godard, P.; Mercier, J. P. *Polym. Eng. Sci.* **1982**, *22*, 229.
- (32) Miley, D. M.; Runt, J. *Polymer* **1992**, *33*, 4643.
- (33) Seefriend, C.; Koleske, J. *J. Macromol. Sci., Polym. Phys. Ed.* **1983**, *21*, 999.

MA0400517